AFRL-RX-WP-TR-2012-0305

IMPACT OF MEDIUM ON THE DEVELOPMENT AND PHYSIOLOGY OF PSEUDOMONAS FLUORESCENS BIOFILMS ON POLYURETHANE PAINT

Wendy J. Crookes-Goodson and Peter A. Mirau
Nanostructured and Biological Materials Branch

Caitlin L. Bojanowski, Michelle L. Kay, and Pamela F. Lloyd
UES, Inc

Andrew Blankemeir and Hamish L. Fraser
Ohio State University

Daniel E. Barlow, Pehr E. Pehrsson, and John N. Russell Jr
U.S. Naval Research Laboratory

D. Matt Eby and Glenn R. Johnson
Applied Microbiology and Biochemistry Branch

FEBRUARY 2012
Final Report

AIR FORCE RESEARCH LABORATORY
MATERIALS AND MANUFACTURING DIRECTORATE
WRIGHT-PATTERSON AIR FORCE BASE, OH 45433-7750
AIR FORCE MATERIEL COMMAND
UNITED STATES AIR FORCE

NOTICE AND SIGNATURE PAGE

Using Government drawings, specifications, or other data included in this document for any purpose other than Government procurement does not in any way obligate the U.S. Government. The fact that the Government formulated or supplied the drawings, specifications, or other data does not license the holder or any other person or corporation; or convey any rights or permission to manufacture, use, or sell any patented invention that may relate to them.

Qualified requestors may obtain copies of this report from the Defense Technical Information Center (DTIC) (http://www.dtic.mil).

AFRL-RX-WP-TP-2012-0305 HAS BEEN REVIEWED AND IS APPROVED FOR PUBLICATION IN ACCORDANCE WITH ASSIGNED DISTRIBUTION STATEMENT.

_____//SIGNED//_____
WENDY GOODSON, Program Manager
Nanostructured and Biological Materials Branch
Materials and Manufacturing Directorate

_____//SIGNED//_____
KATIE THORP, Branch Chief
Nanostructured and Biological Materials Branch
Materials and Manufacturing Directorate

_____//SIGNED//_____
SHASHI K. SHARMA, Deputy Chief
Nonmetallic Materials Division
Materials and Manufacturing Directorate

This report is published in the interest of scientific and technical information exchange, and its publication does not constitute the Government's approval or disapproval of its ideas or findings.

REPORT DOCUMENTATION PAGE

Form Approved
OMB No. 0704-0188

1. REPORT DATE *(DD-MM-YY)*	2. REPORT TYPE	3. DATES COVERED *(From - To)*
February 2012	Final	14 January 2009 – 14 January 2012

4. TITLE AND SUBTITLE

IMPACT OF MEDIUM ON THE DEVELOPMENT AND PHYSIOLOGY OF PSEUDOMONAS FLUORESCENS BIOFILMS ON POLYURETHANE PAINT

5a. CONTRACT NUMBER
In-house

5b. GRANT NUMBER

5c. PROGRAM ELEMENT NUMBER
65502C

6. AUTHOR(S)

Wendy J. Crookes-Goodson, Caitlin L. Bojanowski, Michelle L. Kay, Pamela F. Lloyd, Andrew Blankemeier, Daniel E. Barlow, D. Matt Eby, Glenn R. Johnson, Peter A. Mirau, Pehr E. Pehrsson, Hamish L. Fraser, and John N. Russell Jr.

5d. PROJECT NUMBER
1660

5e. TASK NUMBER
02

5f. WORK UNIT NUMBER
BN124100

7. PERFORMING ORGANIZATION NAME(S) AND ADDRESS(ES)

Nanostructured & Biological Materials Branch
Applied Microbiology and Biochemistry Branch
Air Force Research Laboratory, Materials and Manufacturing Directorate
Wright-Patterson Air Force Base, OH 45433-7750
Air Force Materiel Command, United States Air Force

UES, Inc.
Ohio State University
U.S. Naval Research Laboratory

8. PERFORMING ORGANIZATION REPORT NUMBER
AFRL-RX-WP-TR-2012-0305

9. SPONSORING/MONITORING AGENCY NAME(S) AND ADDRESS(ES)

Air Force Research Laboratory
Materials and Manufacturing Directorate
Wright-Patterson Air Force Base, OH 45433-7750
Air Force Materiel Command
United States Air Force

10. SPONSORING/MONITORING AGENCY ACRONYM(S)
AFRL/RXBN

11. SPONSORING/MONITORING AGENCY REPORT NUMBER(S)
AFRL-RX-WP-TR-2012-0305

12. DISTRIBUTION/AVAILABILITY STATEMENT

Approved for public release; distribution unlimited.

13. SUPPLEMENTARY NOTES

The U.S. Government is joint author of this work and has the right to use, modify, reproduce, release, perform, display, or disclose the work. PA Case Number and clearance date: 88ABW-2012-2622, 2 May 2012. This document contains color.

14. ABSTRACT

Since the 1950s, the Air Force has battled microbial contamination of its fuel systems. Within these systems, microbes are commonly found as biofilms adhered to tank coatings. Thus strategies for mitigating microbial contamination of fuel systems include deterring biofilm growth on coatings. This study investigated how Pseudomonas fluorescens biofilms grow on polyurethane coatings, and contribute to the degradation of those coatings. Specifically, we characterized how medium conditions and substrate composition contribute to growth of P. fluorescens on an antistatic polyurethane coating. We found that P. fluorescens biofilms grew in systems where the only carbon source was the coupon, suggesting that P. fluorescens can use polyurethane as a nutrient source. In addition, we examined the impact of substrate on biofilm growth by quantitating biofilm growth on pigmented and non-pigmented paint. There was no difference in the ability of the biofilm to grow on the pigmented vs. non-pigmented paint, suggesting that the biofilm was utilizing the polyurethane and not the pigment as a carbon source.

15. SUBJECT TERMS

bacteria, biodegradation, biofilms, microbial contaminants, aviation fuel , coating

16. SECURITY CLASSIFICATION OF:			17. LIMITATION OF ABSTRACT:	NUMBER OF PAGES	19a. NAME OF RESPONSIBLE PERSON (Monitor)
a. REPORT	b. ABSTRACT	c. THIS PAGE			Wendy Goodson
Unclassified	Unclassified	Unclassified	SAR	30	19b. TELEPHONE NUMBER *(Include Area Code)* N/A

Impact of medium on the development and physiology of *Pseudomonas fluorescens* biofilms on polyurethane paint

Wendy J. Crookes-Goodson[1*], Caitlin L. Bojanowski[1,2], Michelle L. Kay[1,2], Pamela F. Lloyd[1,2], Andrew Blankemeier[3], Daniel E. Barlow[4], D. Matt Eby[5], Glenn R. Johnson[5], Peter A. Mirau[1], Pehr E. Pehrsson[4], Hamish L. Fraser[3], and John N. Russell Jr.[4]

[1] Nanostructured and Biological Materials Branch, Materials and Manufacturing Directorate, Air Force Research Laboratory, Wright-Patterson AFB, OH 45433
[2] UES, Inc., 4401 Dayton-Xenia Rd., Dayton, OH 43432
[3] Center for Accelerated Maturation of Materials, Department of Materials Science and Engineering, The Ohio State University, Columbus, OH 43210
[4] Surface Chemistry Branch, U.S. Naval Research Laboratory, 4555 Overlook Ave. SW, Washington DC 20375
[5]Applied Microbiology and Biochemistry Branch, Materials and Manufacturing Directorate, Air Force Research Laboratory, Tyndall AFB, FL 32403

* Corresponding Author

Contact information for all authors:

- *Wendy Crookes-Goodson*: AFRL/RXBN, 2941 Hobson Way, Bldg. 653, WPAFB, OH, 45433; 937-255-9385; wendy.goodson@wpafb.af.mil
- *Caitlin Bojanowski*: AFRL/RXBN, 2941 Hobson Way, Bldg. 653, WPAFB, OH, 45433; 937-838-2598; caitlin.knight.ctr@wpafb.af.mil
- *Michelle Kay*: AFRL/RXBN, 2941 Hobson Way, Bldg. 653, WPAFB, OH, 45433; 937-255-9115; michelle.kay.ctr@wpafb.af.mil
- *Pamela Lloyd*: AFRL/RXPJ, 2977 Hobson Way, Bldg. 651, WPAFB, OH, 45433; 937-255-9413; pamela.lloyd.ctr@wpafb.af.mil;
- *Andrew Blankemeier:* Ohio State University, Center for the Accelerated Maturation of Materials, 141 Fontana Labs, 116 W. 19th Ave, Columbus, OH 43210; 740-403-3359; arblank@gmail.com
- *Daniel Barlow*: Naval Research Laboratory, Code 6176, 4555 Overlook Ave SW, Washington, DC 20375; 202-767-2210; daniel.barlow@nrl.navy.mil
- *D. Matt Eby*: AFRL/RXQL, 139 Barnes Dr., Bldg 1117, Suite 2, Tyndall AFB, FL 32403; 850-340-0415; donald.eby.ctr@usl.af.mil

- *Glenn Johnson*: AFRL/RXQL, 139 Barnes Dr., Bldg 1117, Suite 2, Tyndall AFB, FL 32403; 850-283-6223; glenn.johnson@tyndall.af.mil
- *Peter Mirau*: AFRL/RXBN, 2941 Hobson Way, Bldg. 653, WPAFB, OH, 45433; 937-255-8979; peter.mirau@wpafb.af.mil
- *Pehr Pehrsson*: Naval Research Laboratory, Code 6170, 4555 Overlook Ave SW, Washington, DC 20375; 202-767-3579; pehr.pehrsson@nrl.navy.mil
- *Hamish Fraser:* Ohio State University, Center for the Accelerated Maturation of Materials, 141 Fontana Labs, 116 W. 19th Ave, Columbus, OH 43210; 614-292-2708; fraser.3@osu.edu
- *John Russell*: Naval Research Laboratory, Code 6170, 4555 Overlook Ave SW, Washington, DC 20375; 202-767-5879; john.russell@nrl.navy.mil

Abstract

Microbial biofilms cause biodeterioration of polymeric coatings such as polyurethanes. In many cases microbes have been shown to use the polyurethane as a nutrient source. The interaction between biofilms and nutritive substrata is complex, since both medium and substratum can provide nutrients that affect biofilm formation and biodeterioration. Historically, studies of polyurethane biodeterioration have monitored the planktonic cells in the medium surrounding the material, not the biofilm. In this study, we monitored planktonic and biofilm cell counts, and biofilm morphology, in long-term growth experiments conducted with *Pseudomonas fluorescens* under different nutrient conditions. Nutrients affected planktonic and biofilm cell numbers differently, and neither was representative of the system as a whole. Microscopic examination of the biofilm revealed the presence of intracellular storage granules under nutrient poor conditions. These granules are indicative of stress, starvation, and/or entry into stationary phase, which may impact the biodegradative capability of the biofilm.

Keywords

Pseudomonas fluorescens, biodeterioration, biofilms, biofouling, phosphate storage

Introduction

Since the 1950's, microbial contamination of aviation fuel has been a recognized problem (Brown et al. 2010; Rauch et al. 2006). Microbial contamination of fuel can cause clogging of fuel lines, injectors and filters, and degradation of the fuel itself (Brown et al. 2010; Rauch et al. 2006; Falkiewicz-Dulik et al. 2010). In addition, microbial growth can accelerate the degradation of fuel tank coatings and cause corrosion of aluminum and stainless steel tanks and pipelines (Passman 2003). The majority of the biomass (>99%) that contaminates fuel systems exists in biofilms, communities of microbes that live on surfaces and at interfaces (Brown et al. 2010; Branda et al. 2005). Pseudomonad bacteria have been shown to be common constituents of aviation fuel microbiota in numerous studies (Brown et al. 2010; Rauch et al. 2006; Edmonds and Cooney 1967; Ferrari et al. 1998; Gaylarde et al. 1999; Hill 1970). They are avid biofilm-formers and are facultative aerobes that can utilize a large variety of inorganic and organic compounds as nutrient sources (Palleroni and Moore, 2004). Such substrates include polyester polyurethanes (PU) that are often found in fuel tank coatings.

PU is susceptible to microbial degradation via oxidative, hydrolytic, and enzymatic mechanisms (El-Sayed et al. 1996; Gu 2003; Gu et al. 1998; Howard 2002; Howard and Blake 1998; Kay et al. 1991; Nakajima-Kambe et al. 1997; Nakajima-Kambe et al. 1995; Nakajima-Kambe et al. 1999). Pseudomonads and Bacilli have been reported to secrete proteases and esterases that degrade polyurethane (Howard and Blake 1998; Vega et al. 1999; Howard et al. 2001; Blake et al. 1998). The role of biofilm vs. planktonic cells in the enzymatic degradation process is unclear since very few degradation studies have addressed PU-bound cells (Gu et al. 1998; Blake et al. 1998). Gu et al. (1998) grew biofilms on PU in 100% relative humidity over 21 days and found that biofilm cell counts fluctuated greatly over the duration of the experiment, from ~10^4/cm^2 at 3 days, to 10^2/cm^2 at 7 days, to 10^5/cm^2 by day 21. Impedance spectra indicated degradation had occurred in the PU coating after 52 days of exposure, but the authors did not link the biofilm colony forming units CFUs and impedance results. In another study, Blake et al. (1998) did not address biofilms *per se*, but used electrokinetic, electrical impedance, and light diffraction methods to examine the relationship between degradation of colloidal PU particles and their association with *Bacillus* cells. Complexes between PU colloids and bacteria formed within 4-5 h. Beyond 8 h, the number of planktonic cells declined as large (100 μm) aggregrates of PU and bacterial cells formed. The culture stabilized beyond 72 h, leaving portions of the substrate unmetabolized. In a similar study, Howard and Blake (1998) observed that PU degradation occurred despite little attachment of *Pseudomonas fluorescens* to colloidal PU when grown in defined yeast extract salts (YES) medium. However, the kinetics of this degradation relative to other nutrient conditions was not addressed.

Although these studies have addressed biodeterioration as a function of bacterial adhesion to some degree, there is a large gap in understanding the role of biofilms in the PU degradation process. This is particularly evident when one considers that nutrient conditions are determinants of both biofilm formation/dispersion *and* the degradative impact of bacteria on PU substrates. For example, the transition of Pseudomonads from planktonic lifestyles to growth on a surface is triggered by the presence or absence of specific nutrients, as is the transition from monolayer to multilayer biofilms, and the dispersion of mature biofilms (Karatan and Watnick 2009; O'Toole et al. 2000; Sauer et al. 2004).

There is also a link between nutrients and degradation of PU, although the relationship is complex since the bacterial cells can potentially use the substrate as a carbon and nitrogen source (El-Sayed et al. 1996, Nakajima-Kambe et al. 1995). For example, Kay and colleagues (Kay et al. 1991) found that the ability of several environmental bacterial strains to degrade polyester PU foam depended upon the presence of nutrients in the medium. No degradation occurred in minimal salts medium, while degradation was enhanced when yeast extract was included. These studies measured bacterial growth as a function of planktonic growth and did not quantify biofilm growth on the PU substrate, so the role of biofilm in the process is unclear.

To begin to address this knowledge gap, we examined the effects of medium on the development, persistence and physiology of *P. fluorescens* biofilms grown on PU, while simultaneously monitoring planktonic cell numbers. We examined how cell numbers and the physiological state of the biofilms change over the course of a relatively long duration of exposure (28 days) in a closed-loop, flow system. We demonstrate the importance of understanding biofilm physiology when evaluating a bacterium's impact on a potentially nutritive substrate.

Materials and Methods

Coupons

Test samples consisted of 1 X 2 cm aluminum 2024 coupons spray-coated with AS-P108, a commercially available polyurethane topcoat (CAAP Co., Inc., Milford, CT) or neat resin. Coupons were sanded prior to painting to increase adhesion, but no primer was used. All sides and edges were coated to ensure that no metal was exposed.

Microbial exposures

Coupons were exposed in a closed-loop batch flow system consisting of a medium reservoir and capsules linked in series (Fig. 1). The capsule system allowed removal of select coupons per time point without disturbing other capsules/coupons. It also facilitated the maintenance of axenic cultures, as

confirmed by cell plating and SEM microscopy of biofilm and planktonic cultures. The capsules consisted of 15 mm ± 0.25 mm outer diameter glass tubing capped at each end with chromatography column caps (Bio-Rad, Inc.). Each capsule contained 2 coupons (Fig. 1B). Capsules were linked by Tygon® R-3603 tubing.

The main reservoir of the flow system consisted of a side arm flask containing 500 ml of medium that was aerated via a stir bar as well as filter-sterilized air generated from a standard aquarium air pump. Medium was pumped at 0.8 ml/min through the flow system using a peristaltic pump. Prior to inoculation, system components, including pre-assembled coupons in their capsules, were sterilized by autoclaving. Sterile medium was flowed through the system for 24 h before inoculation to ensure that the system had not been inadvertently contaminated. To inoculate the system, a single *Pseudomonas fluorescens* (ATCC #17571) colony was used to start an overnight culture in Luria-Bertani broth. 100 µl of this culture was used to inoculate the flow system. The system was run at room temperature with 0.5X M9 minimal salts medium (Amresco, Inc.), 0.5X M9 minimal salts with 10 mM pyruvate, or yeast extract salts (YES) (Amresco, Inc.) medium. Periodically the system was supplemented with sterile distilled water to accommodate a decline in medium volume due to evaporation.

At each experimental time point, flow was temporarily stopped and individual capsules were removed from the system. Coupons were removed from the capsules using sterile forceps, gently rinsed in 3 ml 0.1 M HEPES (pH 7.3), and immediately processed for cell counting or scanning electron microscopy (SEM). For all types of analysis, the underside of the coupon was assayed so that analysis was performed on adhered biofilm cells, rather than cells that had settled from the medium.

Quantitation of bacterial colony forming units (CFU) on the coupons and in the medium

Biofilm growth on the coupons was quantitated as described previously (Buckingham-Meyer et al. 2007; Herigstad et al. 2001; Zelver et al. 2001). Briefly, coupons were scraped repeatedly into 45 ml of 0.5X M9 medium to remove the adhered biofilm, and then washed with 5 ml of 0.5X M9 medium. The solution was then homogenized for 30 s to disaggregate the bacteria. The cell suspension was serially diluted and plated onto LB-agar by the drop plate method (Herigstad et al. 2001). After incubating at 30° C overnight, colonies were counted and CFUs were calculated per unit area of the coupon. Two coupons were sampled per time point and experiments were performed in triplicate, with the exception of the M9-PYR experiment, which was performed 4 times. Planktonic CFUs were also quantitated by the drop plate method. For quantitation of maximum CFUs and CFUs at day 28, experiments were averaged and standard error of the mean was calculated. The data were subjected to a one-way ANOVA and treatments were compared pairwise using the T-method to determine the statistical significance of the results (Sokal and Rohlf 2012).

Scanning Electron Microscopy (SEM) and Quantitation of Cytoplasmic Granules

Coupons were prepared for SEM microscopy essentially as described in Priester et al. (Priester et al. 2007). Coupons were pre-fixed in 0.075% ruthenium red, 2.5% glutaraldehyde, 50mM L-lysine in 0.1M HEPES, pH 7.3; fixed in 0.075% ruthenium red, 2.5% glutaraldehyde in 0.1M HEPES, pH 7.3; washed three times in 0.1M HEPES, pH 7.3; post-fixed in 2% osmium tetroxide; and rinsed three more times in 0.1M HEPES, pH 7.3. Following staining and fixation, a dehydration series was performed using 30, 50, 70, 80, 90, 95, and two changes of 100% acetone for 10 min each. Samples were then dried through critical point drying (Tsousimis, Inc.) or air drying. Coupons were mounted onto SEM stubs using copper tape. Imaging was performed on an FEI Quanta 600 with a Field Emission Gun. Voltages for the imaging were at 15kV.

For quantitation of cytoplasmic granules, SEM images were taken with the backscatter detector were used. Granules were defined as white, punctate structures within the bacteria. Imaging was performed on monolayer biofilms on 3 areas of one coupon per time point per experiment. Percentages of cells that contained granules were calculated for each image, and weighted averages for each treatment were calculated based on the number of cells counted. Total number of cells quantitated for each experimental time point varied for each experiment, as follows: M9 – pyruvate: 1d, n=462; 28d, n= 615. M9 + pyruvate: 1d, n=261; 28d, n=684. M9 + pyruvate (exchanged): 1d, n=453, 28d, n=516; YES (exchanged): 1d, n=704, 28d, n=260. Data were then subjected to one-way ANOVA. Significance was determined by the Tukey-Kramer procedure for unequal n's (Sokal and Rohlf 2012).

Dual Beam-Focused Ion Beam (DB-FIB) Microscopy and 3-D Reconstruction of the Biofilm

DB-FIB analysis utilized a Helios NanoLab 600 with a liquid gallium ion source and a cold field emission gun for the electron column. The sample was placed on an SEM stub with carbon tape and coated with gold, to help reduce charging from the electron beam. Once the sample was in focus and an area of interest was identified, the sample was tilted to 52°, and a 1 µm thick layer of platinum was deposited on the sample to protect the sample from ion beam degradation during the milling process. The sample was then irradiated with the ion beam in two different processes, trenching on either side of the platinum strap and the serial sectioning of the selected area to allow 3-D reconstruction of the biofilm.

Serial sectioning of the biofilm was carried out with a beam current of 28 pA and an accelerating voltage of 30 kV. Image acquisition was performed in ultra high-resolution mode with a beam current of 86 pA and an accelerating voltage of 1 kV for the electron column. Each slice that was taken in the serial section was 20 nm thick. Three-dimensional reconstructions were rendered utilizing MATLAB-based

software developed by the Center for Accelerated Maturation of Materials at Ohio State University. The program processes the images and Avizo software renders the reconstruction.

Transmission Electron Micrsocopy (TEM) and Energy Dispersive Spectroscopy (EDS)

For TEM, planktonic cells were pelleted, washed twice in cacodylate buffer, and re-pelleted by centrifugation. Once in pellet form, the samples were taken through a TEM fixation and dehydration series, using 2.5% glutaraldehyde in 0.1 M cacodylate buffer and a secondary fixation of 1% OsO_4. In between all steps, the samples were rinsed thoroughly and kept on a rocker. A dehydration series was performed using 25, 50, 70, 95 and three changes of 100% acetone for 30 min each. Samples were embedded in Embed 812 resin. The resulting blocks were ultra-microtomed into 70 nm thick sections with an RMC PowerTome XL Ultramicrotome using a 35^{o} DiATOME diamond knife. Sections were placed onto 3 mm 400 hex mesh Cu grids, dried, stained with uranyl acetate for 15 min, washed thoroughly with double distilled water, and air dried. The grids were then imaged using a Philips CM200 Transmission Electron Microscope equipped with a 4Pi EDS system. For EDS acquisition, the sample holder was tilted ~18^{o} toward the detector and EDS spectra collected for 100 s at approximately 2500 cps. A spectrum was acquired from each of three different areas by placing the probe either on the granules inside the cells, in the cytoplasm but away from the granules, and on the resin itself. Then the spectra from the three areas were compared. Six separate cells were scanned. Counts for each element were normalized to collection time. Since EDS results are strictly qualitative, ratios between each element and carbon were calculated. The means of the elemental ratios and standard error of the means are presented. Significance was determined using the student's t-test.

Results

Biofilm growth and persistence on AS-P108

Previously, *P. fluorescens* has been reported to secrete proteases and esterases that degrade polyurethane (Howard and Blake 1998; Vega et al. 1999). However, these studies were performed on colloidal PU, not PU-coated coupons, and biofilm formation was not assessed. Therefore, we evaluated the ability of *P. fluorescens* biofilms to develop and persist on PU coupons in the presence of various nutrient sources: M9 minimal salts medium, which contains phosphate and ammonium salts, but no carbon source (M9 – PYR); M9 supplemented with 10 mM pyruvate at the start of the exposure period (M9 + PYR); M9 with 10 mM pyruvate, with medium exchanged every 7 days during the exposure period (M9 + PYR (exch)); and YES medium containing glucose, which was also exchanged every 7 days (YES (exch)). Biofilm formation was assessed by plate counting of culturable cells removed from the coupons. When biofilm colony forming units (CFU) were graphed vs. exposure time (Fig. 2A), there

appeared to be differences in biofilm formation and persistence among conditions. However, when we compared the maximum biofilm CFU reached under each condition, none of the conditions was found to be statistically different from the others (Fig. 2C).

While we did not observe statistically significant variation in biofilm formation (higher maximum CFU) based on the nutrients present in the medium, the long-term persistence of the biofilm (CFU at day 28) was significantly affected. For both the M9 - PYR and the M9 + PYR conditions, biofilm CFUs generally declined over 28 days (Fig. 2A), resulting in a statistically significant (P<0.05) difference between the average CFU at day 28 for M9 + PYR (exch) vs. M9 - PYR or M9 + PYR (Fig. 2C). Biofilms cultured in YES medium were not statistically different from M9 + PYR (exch).

In addition to quantifying biofilm CFUs, we also measured planktonic CFUs over the course of the experiment (Fig 2B, D). While the M9 + PYR (exchanged) condition enhanced the biofilm population, it had no effect on the planktonic cell density. Maximum cell density and the density of the planktonic population at day 28 increased only in the presence of YES medium (Fig. 2D). These results demonstrate that medium composition impacts both the biofilm and cell populations, but not in the same way. In addition, carbon is a limiting factor in persistence of *P. fluorescens* biofilms on PU, even though PU is a potential carbon source (El-Sayed et al. 1996; Gu et al. 1998).

AS-P108 is a PU-based paint that contains carbon black particles. Previous research evaluated the growth of biofilms on similar paint but did not evaluate whether the carbon black particles affected biofilm formation or persistence on the paint (Gu et al. 1998). We have observed that *P. fluorescens* readily agglomerates to free carbon black particles when they are added to medium (data not shown). When included in a coating, these particles could change the coating's surface energy or be a potential carbon source for the bacterium, particularly in nutrient poor conditions. To evaluate the contribution of carbon black to biofilm growth and persistence, we compared biofilm CFUs on coupons that were coated with traditional AS-P108 vs. neat resin, i.e., AS-P108 without the carbon black pigment. In our flow system, we found no substantial difference in the biofilm development or persistence on the coupons over 28 d, whether or not the medium contained pyruvate as a carbon source (Fig. 3). This result suggests that carbon black does not affect *P. fluorescens* biofilm formation or persistence on AS-P108.

Effects of medium on biofilm cell morphology and physiology

Scanning electron microscopy performed under high vacuum is known to influence the morphology of biofilm cells and extracellular polymeric substance (EPS), the matrix that holds and protects biofilms (Priester et al. 2007; Carr et al. 1996). Nevertheless, we were able to observe qualitative differences in morphology of biofilms grown under various medium conditions and prepared equivalently for electron microscopy (Fig. 4). Biofilms grown in M9 - PYR lacked EPS and cells often appeared flat

and damaged. Cells grown in M9 + PYR without medium exchange had more extensive EPS networks than those grown in the absence of pyruvate. The EPS appeared as strings, often forming webs around cells. The cells also appeared more cylindrical. Biofilms grown in M9 + PYR with medium exchange had even more extensive EPS than those grown without medium exchange. The EPS appeared to encase the cells in sheets of material, rather than strings. YES-grown biofilm cells appeared cylindrical with less EPS than biofilms grown in M9 + PYR with medium exchange.

In addition to morphological changes to the cells and EPS, we also observed differences in the interior morphology of the cells, specifically the presence or absence of granules (Fig. 4). AS-P018 is a conductive paint, due to the presence of carbon black particles. Usually SEM analysis of biological materials requires sputter coating with conductive particles to limit charging under the electron beam. Because AS-P108 is a conductive substrate, we could image biofilm cells without coating. When imaged this way, the biofilm cells appeared semi-transparent under the electron beam, and granules were readily visible inside many biofilm cells, particularly those grown in M9 medium with or without pyruvate (Fig. 4, top row). These inclusions were also visible in planktonic cells spotted onto conductive tape prior to imaging (data not shown). Since the carbon black particles in the paint also appear white under the secondary electron beam, we evaluated whether biofilm cells had taken up the carbon black particles. Using the SEM backscattered electron imaging, which distinguishes materials based on their atomic (Z) number, we confirmed that the cellular granules had a higher average Z number than the carbon black particles, and therefore had a different elemental composition (Fig. 4, middle and bottom rows).

We used DB-FIB to determine if the particles were inside of the biofilm cells. This technique allows site-specific sectioning of materials through the use of a Ga^+ ion gun, and simultaneous imaging using a scanning electron gun. A day 14 biofilm that had been grown in M9 + PYR was critically point dried and subjected to DB-FIB. A layer of platinum was deposited over the biofilm (Fig. 5A) and the sample was milled with a Ga^+ beam (Fig. 5B). After each 20 nm section, an SEM image was taken of the biofilm (Fig. 5C). These sections clearly revealed the presence of intracellular granules within the biofilm cells. Through advanced segmentation algorithms, we reconstructed the biofilm three-dimensionally (Fig. 5D, E), confirming the intracellular localization of the granules.

When imaging biofilm cells grown in various types of media, we noted a difference in the size and number of cellular granules between time points and treatments. Thus, we quantitated the percent of biofilm cells with granules by counting cells with and without inclusions, as imaged with the backscatter detector (Fig. 6). All day 1 biofilms, regardless of medium type, consisted of approximately 9-18% cells with granules; no statistically significant differences were observed among medium types. However, by 28 days, there was a substantial increase in the number of cells with inclusions in most medium types. In M9 medium with or without pyruvate, 30-50% of biofilm cells contained granules. Biofilms that had

been grown in the presence of YES medium did not show an increase in the percent of cells with granules over the day 1 time point. Thus, although biofilm development did not change substantially with respect to medium (maximum CFUs; Fig. 2C), the morphology of the EPS and quantitation of granules demonstrates that, physiologically, these biofilms are different.

Determination of granule composition by TEM and EDS

Pseudomonads including *P. fluorescens* are known to make several types of intracellular storage granules, including polyhydroxyalkanoates (PHAs), polyphosphates, and sulfur granules, based on nutrient conditions (Haywood et al. 1989; Achbergerova and Nahlka 2011). Therefore, we determined the chemical nature of the cellular granules, to discern what their presence indicates about cell physiology. Since it was technically difficult to create and analyze TEM sections of the intact biofilms on the substrate, we performed the analysis on day 28 planktonic cells. Cells were stained with OsO_4 to enhance contrast within the cells. Inclusions were readily visible in these cells, appearing as spongy, electron dense granules with no surrounding membrane but distinct margins (Fig. 7A). The granules were often unstable under the electron beam. They were similar in appearance to polyphosphate (or 'volutin') granules , as previously described in (Bode et al. 1993; Smith et al. 1954; Schonborn et al. 2001) and did not resemble PHA granules, which are not electron dense (De Eugenio et al. 2010; Sudesh et al. 2000).

EDS was applied to both stained and unstained TEM sections to determine the elemental composition of the granules in comparison to the cytoplasm (Fig. 7B). Five elements (C, O, P, Cu, and Ca) were present in significant quantities. Of these, the Cu signal most likely arises from the TEM grid; EDS spectra of the resin surrounding the cells had equivalent levels of Cu to both the cytoplasm and granules (data not shown). Since EDS is not quantitative among samples without using standards, ratios between each element and carbon were calculated for each sample. Relative to the cytoplasm, the electron-dense granules had elevated levels of P:C,O:C, Ca:C. This elemental composition is consistent with the granules being polyphosphate storage granules, which store energy and chelate metals such as Ca^{2+} (Achbergerova and Nahlka 2011; Schonborn, Bauer and Roske 2001; Kornberg 1995).

Discussion

Biodeterioration of polymeric materials such as polyurethanes is a complex process that is a function of microbial physiology and metabolism, environmental conditions and the chemistry of the substrate. Pseudomonads degrade PU through the activity of membrane bound esterases as well as extracellular proteases and esterases (Howard 2012). The known polyurethanases in *P. fluorescens* are secreted, so biodeterioration facilitated by *P. fluorescens* does not require cellular association with the PU. However, cellular contact, i.e., biofilm formation, could accelerate the degradation process by bringing secreted

enzymes in close contact with the PU. Biofilm EPS, which captures and concentrates biofilm enzymes and signals (Flemming et al. 2007), may also prevent diffusion of polyurethanases into the medium. The relative contributions of biofilm vs. planktonic cells to PU degradation is particularly relevant in industrial settings like pipelines and fuel tanks. In these cases, fluid flow across coatings could carry away enzymes secreted by planktonic cells, limiting their ability to bind to the surface. Thus, by examining both the development and physiology of biofilms grown on PU, we can begin to better understand the impact of biofilms on substrates.

In an experimental system where the substrate is inert, e.g., glass, there is a direct relationship between nutrient levels and the ratio of biofilm:planktonic cells. Biofilms settle and disperse as nutrient conditions change (Karatan and Watnick 2009). However, the relationship between planktonic and biofilm populations becomes more complex when the substrate is a potential nutrient source. Many studies of PU biodeterioration assessed planktonic cell counts to determine how and if the bacteria interact with the substrate. By directly comparing biofilm CFUs with planktonic CFUs under various growth conditions, we showed that planktonic CFUs are not representative of the overall system (Fig. 2).

To quantify biofilm development, we evaluated biofilm CFUs at various time points over a 28 day period, and compared them among various nutrient conditions. CFUs were assessed by counting culturable cells removed from the coupons (Buckingham-Meyer et al. 2007). This method was preferable to confocal microscopy since PU absorbs traditional fluorescent bacterial stains (e.g., live/dead stain), complicating sample analysis and quantitation. Since CFUs do not reflect nuances of cellular physiology, we developed a method to assess the morphology of the biofilm cells, taking advantage of the conductivity of the AS-P108 substrate in imaging. Traditionally, biological samples need to be sputter-coated with conductive nanoparticles to reduce sample charging. Because AS-P108 is conductive, sample coating was not required. Without a coating the biofilm cells appeared semi-transparent, allowing us to observe the presence of cytoplasmic granules. These granules were not visible when the samples were sputter coated with gold (data not shown).

To determine that the granules were inside of, as opposed to underneath, the biofilm cells, we applied DB-FIB microscopy. This technique has been used within the materials science community (Bhandari et al. 2007; Cao et al. 2008), but to date has not been used extensively on biological specimens, except for mineralized materials (Jantou et al. 2009; Mahaney et al.). DB-FIB systems have an ion column with a liquid ion source of gallium (Ga^+) for sectioning, and a Schottky field emission electron column for imaging. This configuration allows site-specific milling of a sample, which is helpful with samples like patchy biofilms. This is in contrast to ultramicrotomy, which is used for traditional TEM sample preparation, where the sample is sectioned and often many sections need to be imaged before the appropriate area of the sample is identified. DB-FIB also permits serial sectioning of the sample,

allowing feature selection, alignment and stacking to reproduce a 3-D reconstruction (Fig. 5). However, like traditional TEM, non-cryo DB-FIB has its drawbacks in that it requires sample dessication prior to milling. Desiccation changes the morphology of the cells, EPS, and overall biofilm, and caution should be exercised when interpreting images (Priester et al. 2007). Nevertheless, in this case it was extremely useful for targeting a particular area of the biofilm, and for determining that the granules observed by SEM were intracellular.

Biofilm CFU counts in different conditions were used to distinguish between biofilm formation and persistence. 'Biofilm formation' was reflected by the maximum CFU's reached during each experiment, and the CFU at day 28 indicated the robustness of the biofilm at the end of the experiment, i.e., the ability of the biofilm to persist on the coupon. Both parameters are important for predicting the relative biodegradative capacity of a biofilm. While graphs of biofilm CFUs vs. time indicated subtle differences in biofilms grown under different nutrient conditions, no statistical differences in biofilm formation were found. The long-term persistence of the biofilm was enhanced in one condition only: M9 + PYR (exch) medium. This result indicated that periodic addition of pyruvate enhanced the ability of *P. fluorescens* to use AS-P108 as a nutrient source, or that it enhanced biofilm formation, or both.

The addition of pyruvate may have enhanced *P. fluorescens*' ability to metabolize PU through increased synthesis of polyurethanases. PU degradation has been shown to be dependent upon nutrient conditions (Kay et al. 1991; Klausmeier 1966; Williams et al. 1969). For example, Kay and colleagues found neither *Corynebacterium* sp. and *Enterobacter agglomerans* could degrade polyester PU foam in minimal medium but degradation was enhanced in the presence of yeast extract (Kay et al. 1991). Similarly, the addition of yeast extract to minimal salts medium enhanced esterase production in fungi (Williams et al. 1969), while the addition of glucose inhibited esterase production in *Corynebacterium* sp. (Kay et al. 1993). Nutrient levels may affect global metabolic regulators that in turn may control the expression, synthesis or secretion of polyurethanases. We did not observe gross morphological damage of the AS-P108 substrate, possibly due to the relatively short duration of the experiment. We independently confirmed that the *P. fluorescens* strain used in this experiment was able to degrade Impranil® PU (data not shown) (Howard et al. 2001).

Nutrient levels may have also affected biofilm formation and physiology regardless of the substratum. There are numerous examples of the relationship between biofilm and nutrients in the literature, and the relationship is complex. In some strains (e.g., *Bacillus subtilis* and *Pseudomonas aeruginosa*) biofilm formation occurs in response to conditions of starvation and may be a survival mechanism during sub-optimal growth conditions (Stanley and Lazazzera 2004). However, in batch *P. fluorescens* cultures, nutrient stress, i.e, depletion of glucose and nitrogen from the medium, leads to detachment of cells from biofilms (Delaquis et al. 1989). In *Pseudomonas putida*, increasing glucose and phosphate concentrations

increased the rate of biofilm formation, but higher concentrations resulted in higher detachment rates, and less biofilm (Rochex and Lebeault 2007). Thus, there may be a fine balance between nutrient conditions and biofilm formation/dispersion.

In our study system, nutrient levels affected biofilm CFUs to some degree, but morphological differences in the biofilm clearly demonstrated that the biofilm cells were physiologically responsive to their environment. Intracellular polyphosphate granules were more numerous in biofilms that were grown in the presence and absence of pyruvate, but not in medium containing glucose (YES). Polyphosphates store energy in cells in the form of energy-rich phophoanhydride bonds (Achbergerova and Nahlka 2011). They regulate many aspects of microbial physiology that are responsive to nutrient availability, including entry into stationary phase, stress and starvation responses, and biofilm formation (Achbergerova and Nahlka 2011; Kim et al. 1998; Potrykus and Cashel 2008). Their appearance in the biofilms suggests that growth conditions were not adequate, even if *P. fluorescens* is capable of utilizing PU as a nutrient source. It also suggests that in the absence of glucose-containing YES medium, the biofilm cells most likely entered a dormant phase. Entry into this phase was further supported by the production of EPS in the M9 + PYR and M9 + PYR (exch) biofilms. EPS production in *P. aeruginosa* increases in stationary phase, and in conditions where nutrients are limited (Kim et al. 1998). The implementation of starvation or stress response could potentially have a major impact on the biodeteriorative capacity of the biofilm, either positively or negatively. A dormant biofilm could potentially protect the substrate from deterioration by more active species. Alternatively, increased synthesis of EPS and its associated enzymes may accelerate deterioration. Future experiments will address the relationship between polyurethanase production, biofilm formation and physiology, and PU biodeterioration.

Acknowledgements

This material is based upon work supported by the Air Force Office of Scientific Research under award number 12RX14COR. The authors thank Dr. Michael S. Goodson for comments on the manuscript.

Distribution Statement A: Approved for public release, distrubution is unlimited., # XXXXXX.

References

Achbergerova L, Nahlka J. 2011. Polyphosphate - an ancient energy source and active metabolic regulator. Microb Cell Fact. 10:63.

Bhandari Y, Sarkar S, Groeber M, Uchic MD, Dimiduk DM, Ghosh S. 2007. 3D polycrystalline microstructure reconstruction from FIB generated serial sections for FE analysis. Comp Mater Sci 41(2):222-235.

Bode G, Mauch F, Ditschuneit H, Malfertheiner P. 1993. Identification of structures containing polyphosphate in *Helicobacter pylori*. J Gen Microbiol. 139:3029-3033.

Branda SS, Vik A, Friedman L, Kolter R. 2005. Biofilms: the matrix revisited. Trends Microbiol. 13(1):20-26.

Blake RC, Norton WN, Howard GT. 1998. Adherence and growth of a *Bacillus* species on an insoluble polyester polyurethane. Int Biodeterior Biodegradation. 42(1):63-73.

Brown LM, McComb JP, Vangsness MD, Bowen LL, Mueller SS, Balster LM, Bleckmann CA. 2010. Community dynamics and phylogenetics of bacteria fouling Jet A and JP-8 aviation fuel. Int Biodeterior Biodegradation. 64(3):253-261.

Buckingham-Meyer K, Goeres DM, Hamilton MA. 2007. Comparative evaluation of biofilm disinfectant efficacy tests. J Microbiol Methods. 70(2):236-244.

Cao S, Tirry W, van den Broek W, Schryvers D. 2008. 3D reconstruction of Ni_4Ti_3 precipitates in a $Ni_{51}Ti_{49}$ alloy in a FIB/SEM dual-beam system. Mater Sci Forum. 583:277-284.

Carr JH, Anderson RL, Favero MS. 1996. Comparison of chemical dehydration and critical point drying for the stabilization and visualization of aging biofilm present on interior surfaces of PVC distribution pipe. J Appl Microbiol. 80(2):225-232.

De Eugenio LI, Escapa IF, Morales V, Dinjaski N, Galán B, García JL, Prieto MA. 2010. The turnover of medium-chain-length polyhydroxyalkanoates in *Pseudomonas putida* KT2442 and the fundamental role of PhaZ depolymerase for the metabolic balance. Environ Microbiol. 12(1):207-221.

Delaquis PJ, Caldwell DE, Lawrence JR, McCurdy AR. 1989. Detachment of *Pseudomonas fluorescens* from biofilms on glass surfaces in response to nutrient stress. Microb Ecol. 18(3):199-210.

Falkiewicz-Dulik M, Janda K, Wypych G. 2010. Handbook of Material Biodegradation, Biodeterioration and Biostabilization. Toronto: ChemTec Publishing.

Ferrari MD, Neirotti E, Albornoz C. 1998. Occurrence of heterotrophic bacteria and fungi in an aviation fuel handling system and its relationship with fuel fouling. Rev Argent Microbiol. 30(3):105-114.

Edmonds P, Cooney JJ. 1967. Identification of microorganisms isolated from jet fuel systems. Appl Environ Microbiol. 15(2):411-416.

El-Sayed AHMM, Mahmoud WM, Davis EM, Coughlin RW. 1996. Biodegradation of polyurethane coatings by hydrocarbon-degrading bacteria. Int Biodeterior Biodegradation. 37(1-2):69-79.

Flemming H-C, Neu TR, Wozniak DJ. 2007. The EPS Matrix: The "House of Biofilm Cells". J Bacteriol. 189(22):7945-7947.

Gaylarde CC, Bento FM, Kelley J. 1999. Microbial contamination of stored hydrocarbon fuels and its control. Rev Microbiol. 30:1-10.

Gu J-D. 2003. Microbiological deterioration and degradation of synthetic polymeric materials: recent research advances. Int Biodeterior Biodegradation.52(2):69-91.

Gu J-D, Roman M, Esselman T, Mitchell R. 1998. The role of microbial biofilms in deterioration of space station candidate materials. Int Biodeterior Biodegradation. 41(1):25-33.

Haywood GW, Anderson AJ, Dawes EA. 1989. A survey of the accumulation of novel polyhydroxyalkanoates by bacteria. Biotechnol Lett. 11(7):471-476.

Herigstad B, Hamilton M, Heersink J. 2001. How to optimize the drop plate method for enumerating bacteria. J Microbiol Methods. 44(2):121-129.

Hill EC. 1970. The control of micro-organisms in aircraft fuel systems. J Inst Petrol. 56(549):138-146.

Howard GT. 2002. Biodegradation of polyurethane: a review. Int Biodeterior Biodegradation. 49(4):245-252.

Howard GT. 2012. Polyurethane Biodegradation. In: Microbial Degradation of Xenobiotics. Berlin Heidelberg: Springer-Verlag.

Howard GT, Blake RC. 1998. Growth of *Pseudomonas fluorescens* on a polyester-polyurethane and the purification and characterization of a polyurethanase-protease enzyme. Int Biodeterior Biodegradation. 42(4):213-220.

Howard GT, Crother B, Vicknair J. 2001. Cloning, nucleotide sequencing and characterization of a polyurethanase gene (pueB) from *Pseudomonas chlororaphis*. Int Biodeterior Biodegradation. 47(3):141-149.

Howard GT, Vicknair J, Mackie RI. 2001. Sensitive plate assay for screening and detection of bacterial polyurethanase activity. Lett Appl Microbiol. 32(3):211-214.

Jantou V, Turmaine M, West GD, Horton MA, McComb DW. 2009. Focused ion beam milling and ultramicrotomy of mineralised ivory dentine for analytical transmission electron microscopy. Micron. 40(4):495-501.

Karatan E, Watnick P. 2009. Signals, regulatory networks, and materials that build and break bacterial biofilms. Microbiol Mol Biol Rev. 73(2):310-347.

Kay MJ, McCabe RW, Morton LHG. 1993. Chemical and physical changes occurring in polyester polyurethane during biodegradation. Int Biodeterior Biodegradation. 31(3):209-225.

Kay MJ, Morton LHG, Prince EL. 1991. Bacterial degradation of polyester polyurethane. Int Biodeterior Biodegradation. 27(2):205-222.

Kim H-Y, Schlictman D, Shankar S, Xie Z, Chakrabarty AM, Kornberg A. 1998. Alginate, inorganic polyphosphate, GTP and ppGpp synthesis co-regulated in *Pseudomonas aeruginosa*: implications for stationary phase survival and synthesis of RNA/DNA precursors. Mol Microbiol. 27(4):717-725.

Klausmeier RE. 1966. The effect of extraneous nutrientees on teh biodeterioration of plastics. SCI Monograph No 23, Microbiological Deterioration in the Tropics:232-243.

Kornberg A. 1995. Inorganic polyphosphate: Toward making a forgotten polymer unforgettable. J Bacteriol. 177(3):491-496.

Mahaney WC, Krinsley D, Langworthy K, Kalm V, Havics T, Hart KM, Kelleher BP, Schwartz S, Tricart P, Beukens R. 2011. Fired glaciofluvial sediment in the northwestern Andes: Biotic aspects of the Black Mat. Sediment Geol. 237(12):73-83.

Nakajima-Kambe T, Onuma F, Akutsu Y, Nakahara T. 1997. Determination of the polyester polyurethane breakdown products and distribution of the polyurethane degrading enzyme of *Comamonas acidovorans* strain TB-35. J Ferment Bioeng. 83(5):456-460.

Nakajima-Kambe T, Onuma F, Kimpara N, Nakahara T. 1995. Isolation and characterization of a bacterium which utilizes polyester polyurethane as a sole carbon and nitrogen source. FEMS Microbiol Lett. 129(1):39-42.

Nakajima-Kambe T, Shigeno-Akutsu Y, Nomura N, Onuma F, Nakahara T. 1999. Microbial degradation of polyurethane, polyester polyurethanes and polyether polyurethanes. Appl Microbiol Biotechnol. 51(2):134-140.

O'Toole GA, Gibbs KA, Hager PW, Phibbs PV, Kolter R. 2000. The Global Carbon Metabolism Regulator Crc Is a Component of a Signal Transduction Pathway Required for Biofilm Development by *Pseudomonas aeruginosa*. J Bacteriol. 182(2):425-431.

Palleroni NJ, Moore ERB. 2004. Taxonomy of Pseudomonads: experimental approaches. In: *Pseudomonas*: Genomics, Lifestyle, and Molecular Architecture. New York: Kluwer Academic/Plenum Publishers.

Passman FJ. 2003. Introduction to Fuel Microbiology. In: Fuel and Fuel System Microbiology: fundamentals, diagnosis, and contamination control. West Conshoshocken, PA: ASTM International.

Potrykus K, Cashel M. 2008. (p)ppGpp: Still Magical? In: Ann Rev Microbiol. Palo Alto: Annual Reviews. p. 35-51.

Priester JH, Horst AM, Van De Werfhorst LC, Saleta JL, Mertes LAK, Holden PA. 2007. Enhanced visualization of microbial biofilms by staining and environmental scanning electron microscopy. J Microbiol Methods. 68(3):577-587.

Rauch M, Graef H, Rozenzhak S, Jones S, Bleckmann C, Kruger R, Naik R, Stone M. 2006. Characterization of microbial contamination in United States Air Force aviation fuel tanks. J Ind Microbiol Biotechnol. 33(1):29-36.

Rochex A, Lebeault JM. 2007. Effects of nutrients on biofilm formation and detachment of a Pseudomonas putida strain isolated from a paper machine. Water Res. 41(13):2885-2892.

Sauer K, Cullen MC, Rickard AH, Zeef LAH, Davies DG, Gilbert P. 2004. Characterization of Nutrient-Induced Dispersion in *Pseudomonas aeruginosa* PAO1 Biofilm. J Bacteriol. 186(21):7312-7326.

Schonborn C, Bauer H-D, Roske I. 2001. Stability of enhanced biological phosphorus removal and composition of polyphosphate granules. Water Res. 35(13):3190-3196.

Smith IW, Wilkinson JF, Duguid JP. 1954. Volutin production in Aerobacter aerogenes due to nutrient imbalance. J Bacteriol. 68(4):450-463.

Sokal RR, Rohlf FJ. 2012. Biometry: the principles and practice of statistics in biological research. 4th ed. New York: W. H. Freeman and Company.

Sudesh K, Abe H, Doi Y. 2000. Synthesis, structure and properties of polyhydroxyalkanoates: biological polyesters. Prog Polym Sci. 25(10):1503-1555.

Stanley NR, Lazazzera BA. 2004. Environmental signals and regulatory pathways that influence biofilm formation. Mol Microbiol. 52(4):917-924.

Vega RE, Main T, Howard GT. 1999. Cloning and expression in *Escherichia coli* of a polyurethane-degrading enzyme from *Pseudomonas fluorescens*. Int Biodeterior Biodegradation.43(1-2):49-55.

Williams PL, Kanzig JL, Klausmeier RE. 1969. Evaluation and production of esterases on plasticizer substrates by fungal spores. Dev Indust Microbiol. 10:177-182.

Zelver N, Hamilton M, Goeres D, Heersink J, Ron JD. 2001. [24] Development of a standardized antibiofilm test. In: Methods in Enzymology: Academic Press. p. 363-376.

Figure Legends

Figure 1. Closed loop batch flow system for coupon exposure.
A, complete system. B, capsule containing 2 coupons.

Figure 2. Impact of nutrient conditions on biofilm and planktonic CFUs.
CFUs from biofilms (A) and planktonic cells (B) grown under various medium conditions. Each experimental replicate is shown. Error bars are standard error of the mean. C, D, Average maximum CFUs (*Max CFU*) and CFUs at completion of experiment (*CFU at day 28*) for biofilms (C) and planktonic cells (D), shown in A and B, respectively. *M9 – PYR*, M9 salts without pyruvate; *M9 + PYR*, M9 salts with 10 mM pyruvate; *M9 + PYR (exch)*, M9 + PYR with medium exchange every 7 d; *YES (exch)*, YES medium with medium exchange every 7 d. Data are means ± s.e.m. (+) indicates significant (P<0.05) difference compared to M9 - PYR (T-method). (*) indicates significant (P<0.01) difference compared to all other treatments (Tukey-Kramer method).

Figure 3. Biofilm growth and persistence on pigmented vs. non-pigmented PU.
A, CFUs from biofilms grown on PU with (*Paint*, closed symbols) and without (*Neat*, open symbols) carbon black, in M9 minimal medium without (*M9 – PYR*) and with (*M9 + PYR*) pyruvate. Each replicate experiment is shown for each condition; data from Fig. 2A are re-plotted on this figure to ease comparison. B, Average maximum CFUs (*Max CFU*) and CFUs at completion of experiment (*CFU at 28d*) for biofilms from experiments shown in A. Data are means ± s.e.m

Figure 4. SEM of biofilms and quantitation of intracellular inclusions. A, SEM of inclusions formed in biofilm cells on painted coupons. *Top row*, SEM images of day 28 biofilms taken with an Everhart-Thornley secondary electron detector . Scale bar = 3 μm. *Middle row*, samples in top row re-imaged with the SEM back scatter electron detector . Scale bar = 3 μm. *Bottom row*, magnifications of boxed regions in middle row. Scale bar = 0.5 μm. *Large arrowheads*, carbon black particles. *Small arrowheads*, inclusions. Biofilms were grown under various medium conditions as indicated.

Figure 5. DB-FIB analysis of *P. fluorescens* biofilm on polyurethane paint. A, SEM image of a 14d biofilm overlayed with platinum (Pt). Scale bar = 10 μm. B, Sample after trenching on either side. Scale bar = 30 μm. C, Higher magnification image of the biofilm after milling. Scale bar = 20 μm. *Yellow arrowhead*, intracellular granule. D, 3-D reconstruction of the biofilm cells (dark blue) with multicolored granules. E, Single *P. fluorescens* cell showing granules.

Figure 6. Quantitation of intracellular inclusions. Percent of biofilm cells with inclusions after 1 and 28 days of exposure to *P. fluorescens*, under medium conditions indicated. Data are weighted means ± s.e.m. (*) indicates significant (P<0.05) difference compared to all other treatments (Tukey-Kramer method).

Figure 7. Microscopic and spectroscopic analysis of inclusions in cells. A, TEM of planktonic *P. fluorescens* with granules. *Left*, scale bar = 1 μm. *Right*, scale bar = 400 nm. Arrows indicate where spectra were taken on sample. *White arrow*, granule. *Black arrow*, cytoplasm. B, EDS analysis of the granules. Raw counts for each element were normalized to collection time. *O*, oxygen; *C*, carbon, *P*, phosphate, *Ca*, calcium. Data are means ± s.e.m., n=6. (*) indicates significant ($P < 0.05$) difference compared to cytoplasm (two-sample t-test). (+) indicates significant ($P < 0.005$) difference compared to cytoplasm (two-sample t-test). *ND*, not detected. *Granule* and *Cytoplasm* are represented by arrows in panel A.

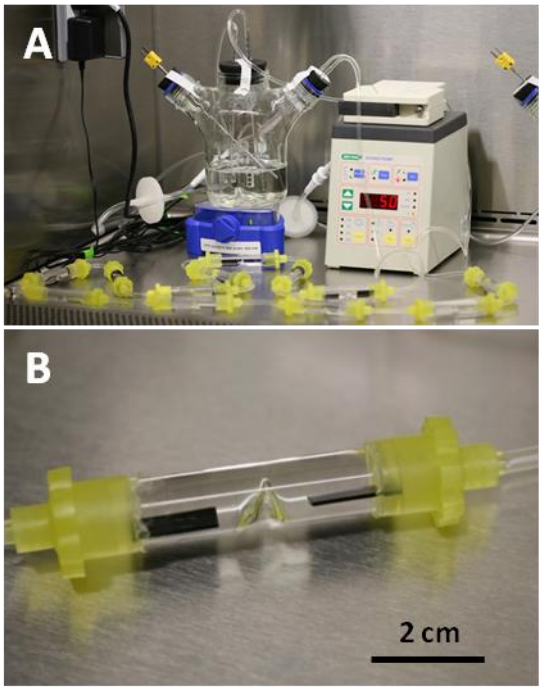

Figure 1.

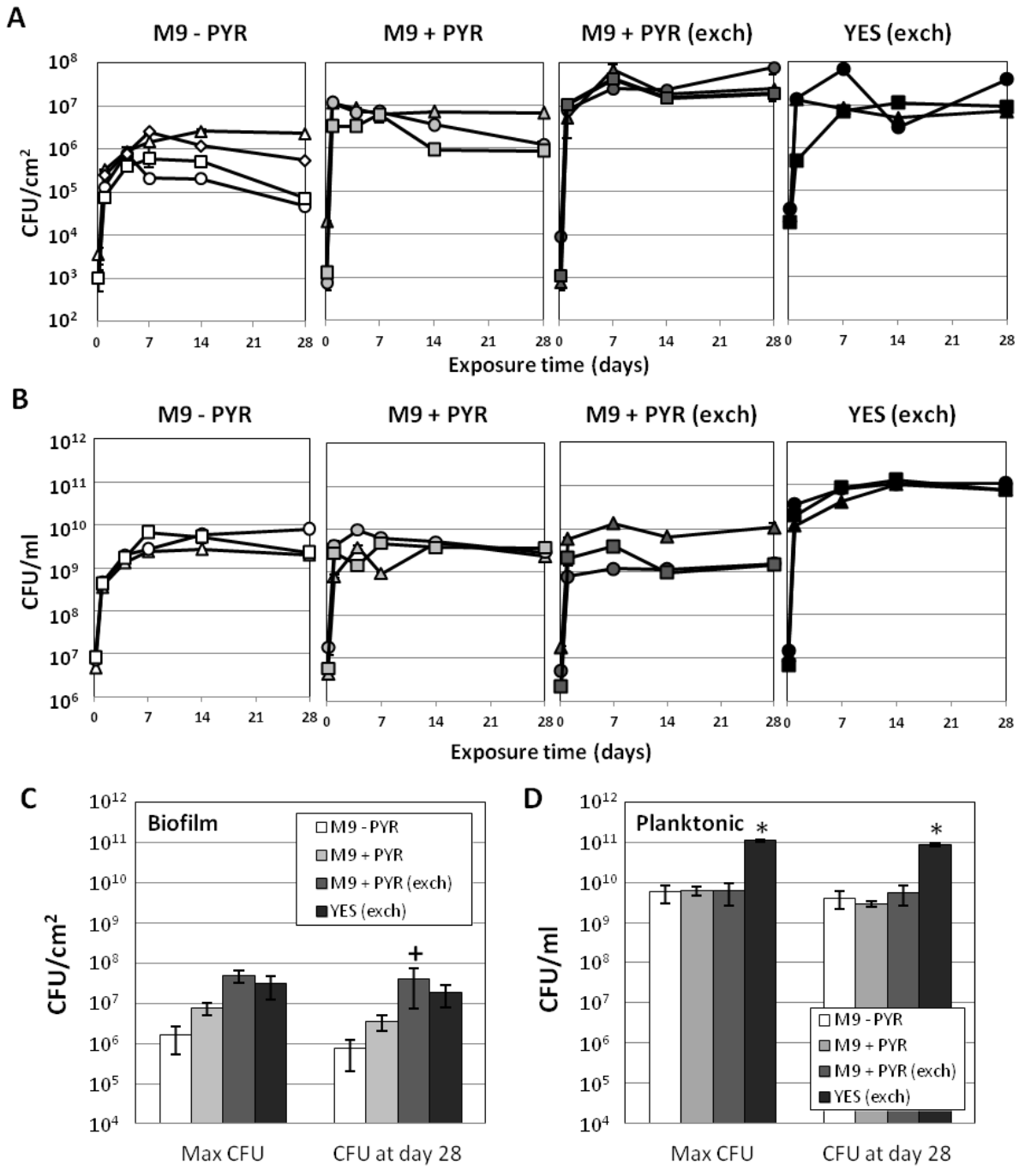

Figure 2.

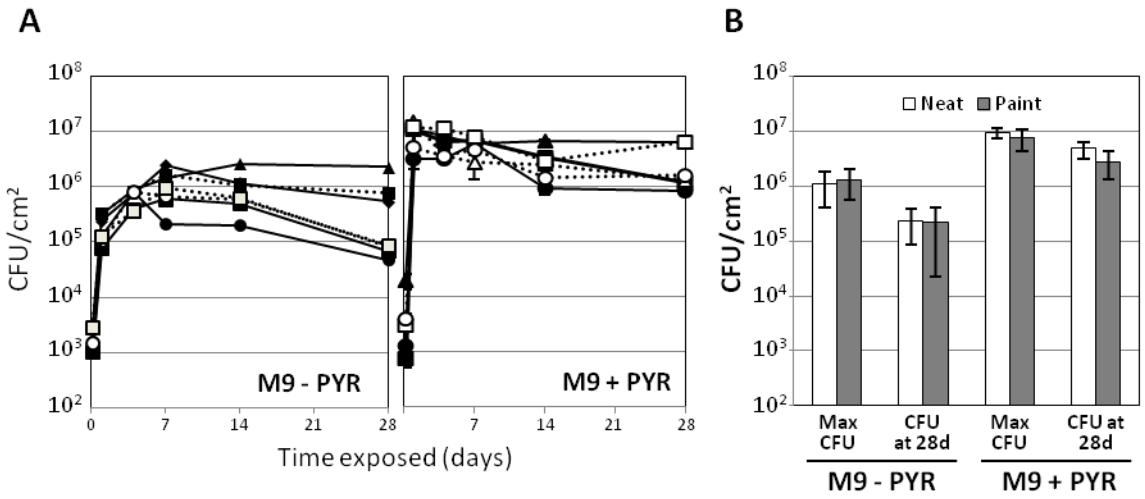

Figure 3.

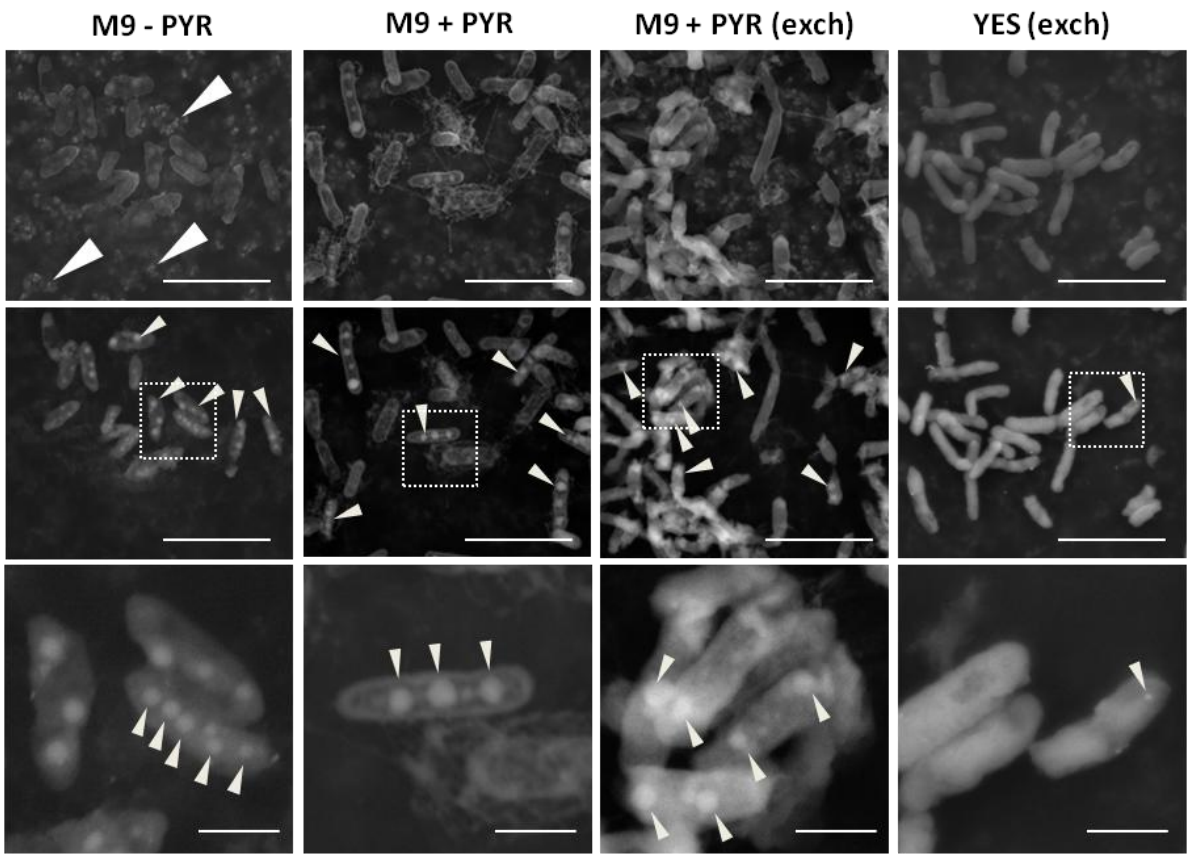

Figure 4.

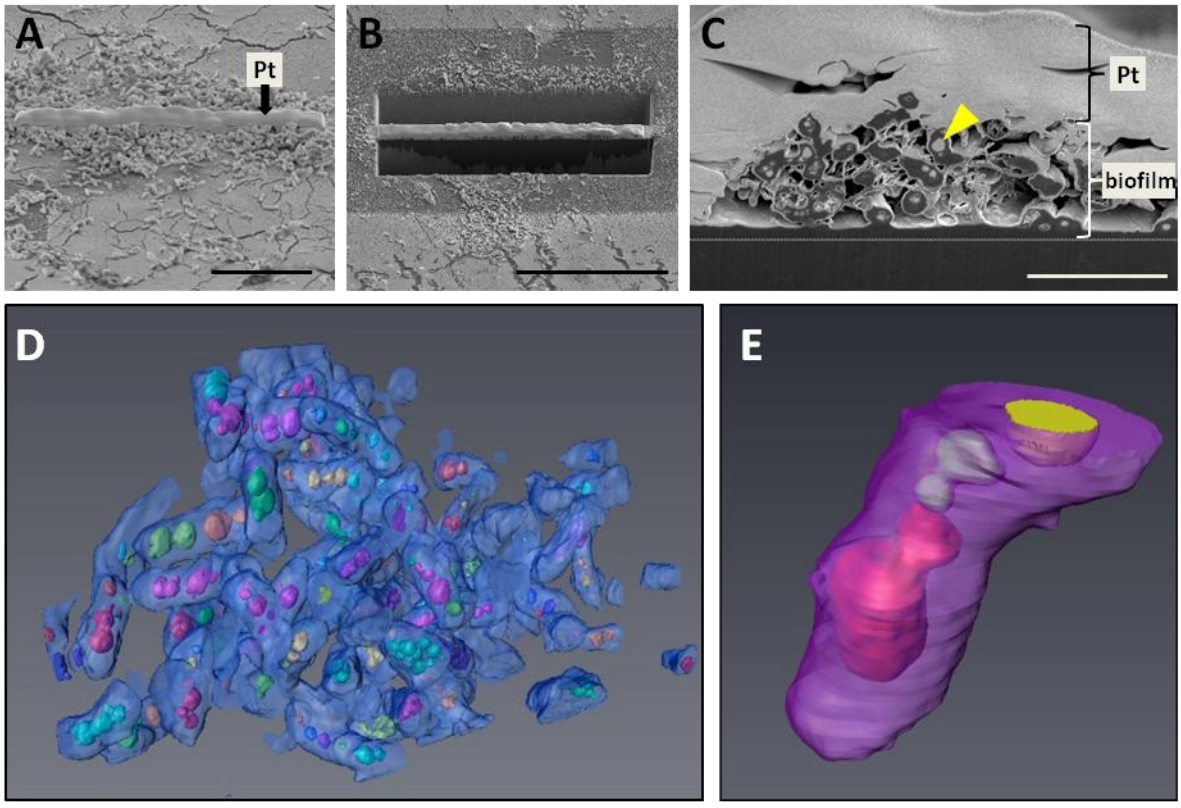

Figure 5.

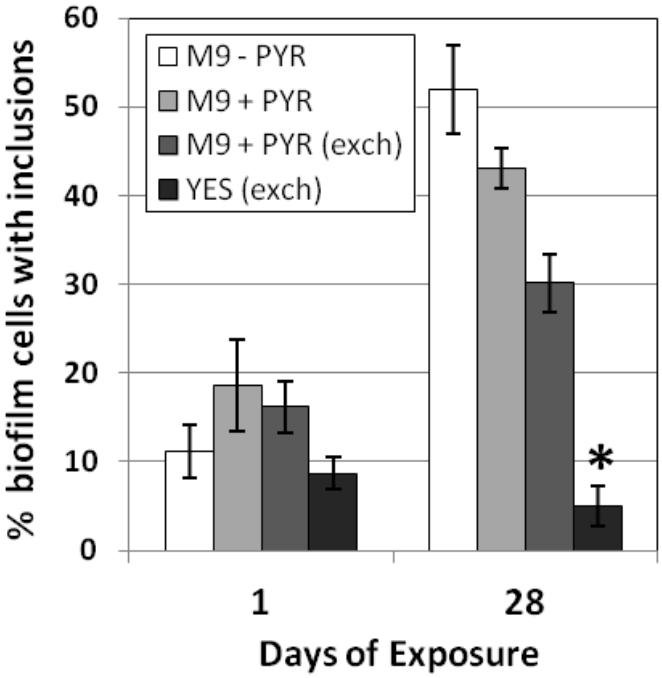

Figure 6.

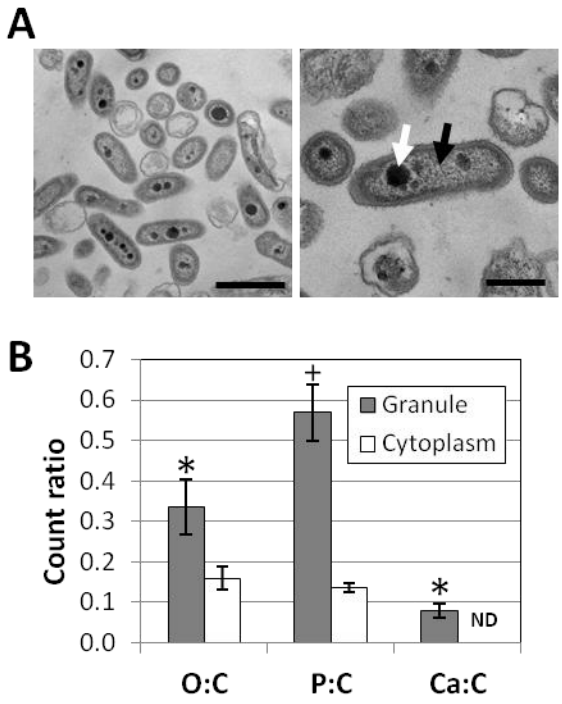

Figure 7.